Egyptian Geophysical Society
EGS Journal, Vol. 14, No. 1, 131-141 (2016)

SHALLOW GEOPHYSICAL TECHNIQUES FOR GROUNDWATER AQUIFER EXPLORATION, AIN ALSOKHNA AREA, WEST GULF OF SUEZ, EGYPT

A.A.A. Othman[(1)], Th.H. Abd El-Hafez[(1)], M.A.S. Youssef [(2)] and M.E.M. Sabra[(3)]

(1) Geology Department, Faculty of Science, Al-Azhar University, Cairo, Egypt.
(2) Nuclear Materials Authority, Exploration Division, P. Box 530, Maadi, Cairo, Egypt.
(3) Egyptian Mineral Resources Authority, P. Box 11517, Abbasiya, Cairo, Egypt.

استخدام الطرق الجيوفيزيقية الضحلة لاستكشاف خزانات المياه الجوفية، العين السخنة، غرب خليج السويس، مصر

الخلاصة: اهتم البحث بدراسة تكاملية للمسوحات السيزمية والكهربية وسبر الآبار معاً للمنطقة محل الدراسة وذلك لتحديد مستوى خزانات المياه الجوفية بمنطقة الدراسة والمواقع المناسبة لحفر آبار لهذه المياه الجوفية. تم تطبيق طريقة المسح السيزمى الضحل وفى إطار هذه الطريقة، تم عمل ٨ خطوط سيزمية بطول ١٢٠ متر وقد تبين سرعة الموجات الأولية للطبقات التحتسطحية كالآتى: الطبقة لأولى وتمثل طبقة الرواسب الوديانية المفككة حيث تتراوح السرعة بداخلها من ٥٠٠ إلى ٦٢٥ م/ث و يتراوح سمك هذه الطبقة من ١ إلى ٣,٥ متراً وأما الطبقة الثانية فتمثل طبقة الرواسب المتماسكة وتتراوح السرعات بهذه الطبقة من ١٣٠٠ إلى ١٦٠٠م/ث ويتراوح سمكها من ٩,٥ إلى ٢٧,٥ متراً، أما الطبقة الثالثة فتمثل طبقة الحجر الرملى حيث تتراوح السرعات فى هذه الطبقة من ٢٤٠٠ إلى ٣٠٠٠ م/ث. وتعطى السرعات الأولية للطبقات التحتسطحية السالفة الذكر مؤشرا جيداً على تواجد المياه الجوفية بالطبقة الثانية والثالثة كما تم تطبيق طريقة الجس الكهربى الرأسى بجوار الآبار ذات التسجيلات الجيوفيزيائية حيث تم عمل خمس جسات كهربية بالقرب من الآبار كما ظهرت مواقع الجسات الكهربية الخمسة كالتالى: الجسة الكهربية الأولى تقترب من البئر الرابع والجسة الثانية تقترب من البئر الأول أما الثالثة فتقترب من البئر الثالث والجسة الرابعة فقريبة من البئر الثانى كما تم عمل عدد (٢) قطاع جيوكهربى حيث يمر القطاع الأول بالجسة الأولى والثالثة والخامسة على الترتيب، أما القطاع الثانى فيمر بالجسة الثانية والثالثة والرابعة على الترتيب. وقد أظهرت نتائج الجسات الكهربية أربعة طبقات تحتسطحية هى كالتالى: طبقة الرواسب الوديانية – طبقة الرمال المفككة – خزان المياه الجوفى والذى يشمل الطبقة الثالثة والرابعة بحيث تزيد متوسط قيمة المقاومة الكهربية النوعية للطبقة الأولى والثانية عن ٤٤٠ أوم. متر، أما الطبقة الثالثة والرابعة فتبلغ قيمة المقاومة الكهربية النوعية بهما أقل من ٢١ أوم. متر وهى مؤشر جيد على تواجد خزان المياه الجوفية. تم تحليل نتائج التسجيلات الجيوفيزيائية للآبار باستخدام قياس أشعة جاما الطبيعية، الجهد الذاتى، المقاومات الكهربية، تسجيلات الكثافة والتسجيل النيوترونى حيث أوضحت هذه القياسات النوعيات الصخرية المختلفة بمنطقة الدراسة والتى هى غالباً أنواع مختلفة من طبقات الحجر الرملى كما أظهرت المستوى السطحى للمياه الجوفية عند أعماق ١٧، ٤٠، ١٥ و ٤٥ مترا بالآبار ١، ٢، ٣ و ٤ على الترتيب. وبمقارنة النتائج السابقة للطرق الجيوفيزيائية المختلفة، أظهرت هذه النتائج تقارباً كبيراً حيث أوضحت النوعية الصخرية للطبقات التحتسطحية (الرواسب الوديانية والرمال المفككة – الرواسب المتماسكة– طبقة الحجر الرملى) كما بينت المستوى السطحى للمياه الجوفية بالمنطقة حيث يزداد باتجاه الغرب ويقل كلما اتجهنا ناحية الشرق وأخيراً معرفة مواقع حفر آبار المياه الجوفية المناسبة وتمثل الجسات السالفة الذكر مواقع متميزة وخصوصاً الجسة الثانية.

ABSTRACT: *Eight seismic refraction profiles, five vertical electrical soundings (VES) and four geophysical well logging tools were acquired along the western side of Gulf of Suez, Egypt, in order to study the aquifer's geometry, groundwater level, and locate promising sites for future water drilling wells. The well logging measurements included natural gamma ray (GR), self potential (SP), electric resistivity (16" and 64"), density and neutron. The seismic primary wave velocity distribution different velocities ranging between 500 – 625 m/s, 1300 – 1600 m/s and 2400 – 3000 m/s. The obtained results showed that the first low velocity range may indicate non-saturated zone which is directly affected by surface water that appears along the studied area. The second and third velocities ranges may show water level at saturated zone and the lithologic interfaces. The estimated thickness of the unsaturated zone varies between 1 m and 3.5 m. The thickness of the top saturated zone ranges between 9.5 m and 26 m which represent the gradual increase of seismic velocity layers with depth. This increase may be due to the dense rocks which change vertically from alluvial at the surface to compacted sediments and then to sandstone at depth. The true resistivities of the aquifer show two zones; the first zone is a surficial resistive layer of dry alluvium, unconsolidated with consolidated Wadi sediments, which have average resistivity of more than 440 Ω.m then lower resistivities reaching to 21 Ω.m in the second zone which constitutes the main aquifer in the third and fourth geoelectric layers.*

The geophysical well logging tools confirmed the water depths obtained from the seismic refraction analysis and vertical electrical soundings. The water table levels start below 17, 40, 15 and 45 m at wells no. 1, 2, 3 and 4, respectively. In addition, they give more detailed explanation about the subsurface lithologies and their physical properties through varying lithologies with depth such as porosity, clean or radioactivity, density and electrical resistivity. The integration of these results confirms the existence of a groundwater aquifer within this interval. The combination between the three executed geophysical methods indicated that the subsurface lithology of the area is composed of three layers. The first top layer is formed from unconsolidated and consolidated Wadi sediments (non-saturated zone) and the second saturated zone is a fractured rock composed mainly of saturated sandstone and

considered a promising layer for groundwater accumulation. The surface level of groundwater was increased toward the west and decreased toward the east of the studied area. The obtained results show that for any future drilling for groundwater, a number of VES positions may be considered as potential locations, especially at VES 3.

INTRODUCTION

Groundwater resources play a vital role in the spreading of urbanization and encouragement of investments in Ain Alsokhna area. Consequently, groundwater resources of Ain Alsokhna area were intensively investigated by many workers (Eldiasty et al., 1981; Abuelata and Hassanan, 1990; Abdellateif et al., 1997; Elbeheiry et al., 2004) and many others).

The seismic refraction method and the vertical electrical sounding (VES) method are important geophysical methods. They were adopted to investigate the probability of fresh groundwater occurrences in the studied area. The objective of the seismic and geoelectric measurements is to confirm or not this assumption that, the groundwater accumulation can primarily be revealed by seismic refraction technique, especially in the gravely-sands or silty clay areas, in which the groundwater level can be defined as a boundary of acoustic impedance (Galfi and Palos, 1970). Shallow seismic survey can be very useful when integrated with vertical electrical sounding (VES) and confirmed by well logging measurements, in order to investigate changes in the groundwater level and possibly locate the fresh groundwater aquifer and other promising sites for future drilling of wells in the studied area.

Location and Geologic Setting

Ain Alsokhna area is a region in the Suez Governorate and is located on the western side of Gulf of Suez, Egypt (Fig. 1). Geomorphologically, Ain Alsokhna area is divided into four main units (Conoco; 1987; Salem, 1988 and Said, 1990), as follows:1) Coastal plain unit; It is represented by a low land that occur between Gulf of Suez to the east and a hilly and mountaineous terrain further west. It is mainly covered by Quaternary clastic, extensive thick gravely and sandy sediments, forming a gently seaward sloping plain. 2) A high land unit; It is represented by Gabal Ataqa, Northern Galala, and the plateaus. Gabal Ataqa is a bold mountain block forming high vertical scarps (their northern and eastern sides) reaching highest point of about 900 m above sea level, and the Northern Galala which represents a great massive block situated in the northern part of the Gulf of Suez.3) A low lying hill unit; It is mainly covered by Upper Eocene, Oligocene and Miocene rocks.4) The drainage pattern; It is defined by four major drainage basins in Ain Alsokhna area. These basins from north to south are: Wadi Hagoul and then Wadi located to the south of Wadi Hagoul, Wadi Akheider bada and Wadi Ghoweibba.

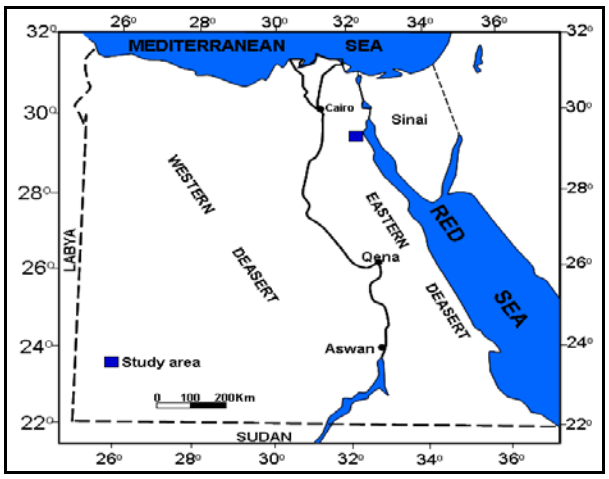

Fig. 1: Location map of Ain El-Sokhna area, Egypt.

Regional lithologic units and structures were observed and investigated thoroughly in the field, as shown on Fig. (2). Abu-Elenain and Ismail, (1995) divided the Eocene rocks into; Middle Eocene (Mokattam Formation) and Upper Eocene (Maadi Formation). The Oligocene rocks uncomfortably overlie the Upper Eocene clastics. Oligocene rocks appear in two different types: volcanic rocks (basaltic sheets and doleritic intrusions), which overlie the Upper Eocene clastic rocks, and sedimentary rocks (sandstone, quartizite and flinty gravels), which are overlain by the Lower Miocene rocks. Miocene rocks consist, from top to bottom, as follow: Hagoul Formation (Upper Miocene) and Sadat Formation (Lower Miocene). The Pliocene sediments consist mainly of a series of gravels and flint pebbles in a sandy matrix, meanwhile in some other parts, these gravels consist of a mixture of flint and limestone pebbles as well as in a sandy matrix (Salem, 1988). Quaternary sediments are represented by Holocene and Pleistocene, which are made up of gravels, cobbles, boulders and sands in the form of Quaternary terraces and alluvium.

Youssef and Abdel Rahman (1978) considered the studied area as a huge graben, in which numerous gently tilted fault blocks protrude above the general surface. Salem (1988) analyzed the structural features of the studied area to identify its deformational style that affected the area and the probable stress directions. He also pointed out the relation between the style of deformation and two provinces (Gulf of Suez to the east and the Cairo-Suez district to the north). He mentioned that the majority of the faults are normal and few of these are diagonal-slip, with major dip-slip and minor strike-slip components.

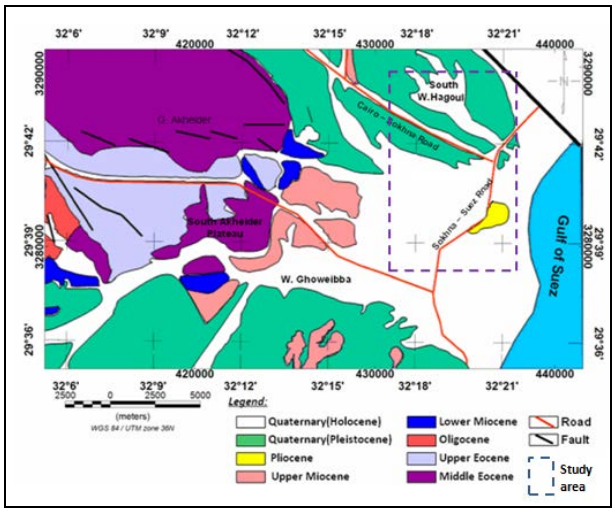

Fig. 2: Regional geologic map of the studied area (after, Conoco 1987).

METHODOLOGY AND DATA ACQUISITION

Shallow Seismic Refraction Survey:

Seismic refraction method uses the seismic energy that returns to the surface after traveling through the ground along refracted-ray paths. The first arrivals of the seismic energy, to a detector offset from a seismic source, always represent either a direct-ray or a refracted-ray (Reynolds, 1997). The compressional wave velocity increases the confining pressure. The sandstone and shale velocities show a systematic increase with depth of burial and with age, due to the effects of progressive compaction and cementation. Shallow seismic survey was carried out using a seismograph Model-1125E McSEIS-SX, 12, highly sensitive vertical geophones and a sledge hammer energy source of 10 kg. Two off-end spreads (forward and reverse) were designed for this survey, according to the available geological information and the main aim of the study.

Eight seismic refraction profiles were acquired in the studied area. The profile extensions were 120 meters in length and trend in the NW-SE direction. Forward, reverse, split and offset seismic shootings were carried out with a geophone interval of 10 meters. The locations of these profiles in the studied area are shown on a map of (Fig. 3).

The seismogram is the main result of field work. It represents the analog recording of the received signals. The recorded seismic traces reflect the responses of the subsurface interfaces. Figure (5A) shows an example of the seismogram of a split shot of the first spread. The most important first arrivals are the direct and refracted waves, were received by the geophones. Some of the recorded traces were noisy or bad traces, even after applying filtering techniques during processing stage, which was carried out to enhance the signal/noise ratio. These bad or high noisy traces were discarded or deleted from some of the shot records.

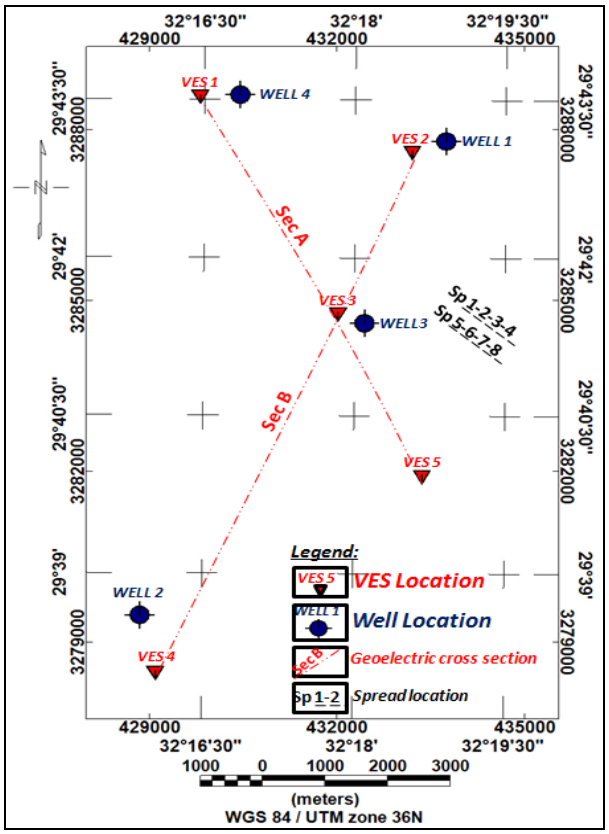

Fig. 3: Location map of seismic refraction spreads, VES, geoelectric cross section and Drilled wells of the studied area.

The picked first-arrival times are converted into corresponding depth-velocity sections (geoseismic cross sections) using Winsism 9 software (2009), based on the Generalized Reciprocal Method (GRM).

Vertical Electrical Sounding (VES):

Resistivity surveys measure the composite electrical resistivity of the subsurface. A direct current is induced into the ground between two current electrodes A and B, and the potential difference is measured between two potential electrodes M and N (Fig. 4). A resistance value is obtained by dividing the measured voltage (V) by the induced current (I). The apparent resistivity is calculated from the resistance value and geometrical factor, that accounts for the electrode spacing configuration.

In the present study, the electrical resistivity measurements were carried out using Schlumberger array configurations (Zohdy, 1974). This array remained as one of the best arrays for depth sounding among the different array configurations. The main application of this array is to explore the groundwater aquifer occurrences. In this method, the center point of the electrode array remains fixed, but the spacing between electrodes are increased progressively to obtain more information about the deeper sections of the subsurface (Fig. 4).

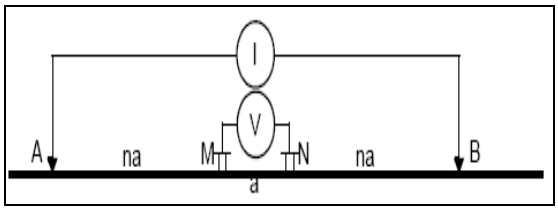

Fig. 4: Sketch diagram showing the Schlumberger electrode arrays.

The Vertical Electrical Sounding (VES) survey was conducted at 5 sites distributed in the studied area (Table 1 and Fig. 3). The VES specifications were selected as seven measurements per decade to obtain excellent data continuity, while half current electrode spacing (AB/2) started from one meter to 500 meter. The equipment used in the present study is ELREC-T, IRIS Instruments, France, with a microprocessor, digital display and RS-232C interface for the PC data dump. From the field data, the apparent resistivities (ρ_a) were plotted versus AB/2 on a log-log paper. The advantages of log-log plot is that, it emphasizes the near-surface resistivity variations and suppresses the variations at greater depths. This is important, because the interpretation of the results depends largely on small variations in the resistivities occurring at shallow depths.

Table (1): 5 VES locations in the studied area.

VES No.	Coordinates			
	Lat / long		UTM	
1	29° 43′ 32″ N	32° 16′ 27″ E	429804 E	3288618 N
2	29° 43′ 01″ N	32° 18′ 33″ E	433198 E	3287633 N
3	29° 41′ 26″ N	32° 17′ 56″ E	432175 E	3284726 N
4	29° 38′ 04″ N	32° 16′ 02″ E	429080 E	3278507 N
5	29° 39′ 56″ N	32° 18′ 40″ E	433353 E	3281945 N

The VES field data were interpreted through successive interpretation steps. Feeding the field data to a PC represents the first step, in order to get the n-layer model. The interpretation of the VES was obtained through using an automatic interpretation multi-layer computer program (Zohdy and Bisdorf, 1989). Based on these interpretations, the parameters of ρ (resistivity), d (depth) and h (thickness) of a geoelectric model, thought to be closer to reality, were estimated.

Geophysical Well Logging:

Four wells were drilled by the Egyptian Geological Survey and Mining Authority (EGSMA), in the studied area. They are located near the seismic refraction survey and VES area (Fig. 3). They showed the different types of layers within the area under examination. Well logging measurements included in Natural Gamma ray (GR) for measuring total radiation and Self Potential (SP) for delineating line base mud and lithologic contacting, electric Resistivities (16″& 64″), for measuring the resistivities of the flushed zone, and the true formation respectively, Density log for displaying rock density and Neutron log, that illustrates the rock porosity.

DISCUSSION

The results obtained from shot records (Table 2) and their interpretations indicate that the P-wave velocities can be determined as:1) Unconsolidated Wadi sediments at the top having P-wave velocities range of (V_{p1}=500 - 625 m/s), in which the thickness of this layer varies between 1.0 and 3.5 m.2) The second layer velocities range of (V_{p2}=1300-1600m/s), which corresponds to consolidated Wadi sediments and show the surface of water at this layer. The thickness of this layer varies between 9.5 and 26 m. 3) The third layer is characterized by high average seismic velocity ranges of V_{p3}=2400-3000 m/s, that corresponds to fractured sandstone layer.

These velocity ranges may represent the bed interfaces. It is noticed that, the refracting velocity at the water level is the lowest when the water level is at the shallowest depth. When the water level drops closer to the top of the saturated zone, refracting velocities are observed to increase. However, as the water level drops close to the saturated zone, it may become undetectable. One example of seismogram of split shot and the time-distance curve of the first spread in the studied area is shown on Fig. (5 A and B) and the eight geoseismic cross sections in the studied area which reflect three main seismic layers (Fig. 6A to 6H).

The resultant multi-layer model for VES (1), using Ato program (Zohdy and Bisdorf, 1989), is shown as an example is shown in (Fig. 7A). It represents the initial model used for feeding the Resist layering program (Velpen, 1988) and constructing the subsurface true resistivity contour sections. The five layering models of Resist program (Figs. 7B to 7F) were used to reduce the layers to 4, in order to build up a geoelectric model. The results of these VES are resistivity, thickness and depth, as summarized in Table (3).

According to the behaviour of field curves and the number of subsurface geoelectric layers for each sounding, VES results indicate that the true resistivities of the shallow section reflect first a surficial resistive layer of dry alluvium with a resistivities ranging between 440 and 3600 Ω.m, then a lower resistivty, which reaches 440 Ω.m at VES 5, followed by the highest resistivity, which attains 3655 Ω.m at VES 2. The second geoelectric layer is characterized by gravel, sand and loose sand, which possesses an average resistivity of 200 Ω.m and an average depth of 2.5 m. The third and fourth geoelectric layers represent the best aquifer, which have low resistivity values of less than 100 Ω.m. According to Bernard (2003), in order to identify the presence of groundwater from resistivity measurements, one can look to the absolute value of the ground resistivity: for a practical range of fresh water resistivity of 10 to 100 Ohm.m.

Table 2: Velocity parameters of the geoseismic layers.

Spread No.(Sp)	(GI)&(SL) and (DS)	Character of layer	Geoseismic Layers (GSL)		
			Layer (1)	**Layer (2)**	**Layer (3)**
Sp 1 (Fig. 6A)	10&120m (NW-SE)	Velocity (m/s)	550 - 625	1350 - 1550	2300 - 2600
		Thickness (m)	1.3 - 2.5	17 - 19	------
		Top of layer (m)	12 - 16	11 - 13.5	(-4.5) - (-7)
Sp 2 (Fig. 6B)	10&120m (NW-SE)	Velocity(m/s)	550 - 600	1400 - 1600	2600 - 3000
		Thickness(m)	1 - 2.5	15.5 – 18	------
		Top of layer (m)	11 - 17.5	10 - 13	(-3) - (-8)
Sp 3 (Fig. 6C)	10&120m (NW-SE)	Velocity(m/s)	500 - 600	1400 - 1550	2200 - 2600
		Thickness(m)	1 - 2.5	18 - 26	------
		Top of layer (m)	15.5 - 19	15 - 18	(-1) - (-8)
Sp 4 (Fig. 6D)	10&120m (NW-SE)	Velocity(m/s)	550 - 600	1400 - 1600	2200 - 2600
		Thickness(m)	1 - 2	20.5 - 24.5	------
		Top of layer (m)	15 - 18	14 - 17	(-4) - (-8)
Sp 5 (Fig. 6E)	10&120m (NW-SE)	Velocity(m/s)	500 - 600	1300 - 1500	2600 - 2900
		Thickness(m)	2.5 - 3.5	9.5 - 12.5	------
		Top of layer (m)	17.5 - 20	14 - 16	2.5 - 6
Sp 6 (Fig. 6F)	10&120m (NW-SE)	Velocity(m/s)	550-600	1300 - 1500	2400 - 2600
		Thickness(m)	1 – 1.5	17 - 23	------
		Top of layer (m)	14 - 18	12.5 - 15	2 - (-8)
Sp 7 (Fig. 6G)	10&120m (NW-SE)	Velocity(m/s)	500 - 600	1400 - 1600	2200 - 2600
		Thickness(m)	1.5 - 2.4	17 - 26	------
		Top of layer (m))	19 - 23	18 - 21	2 - (-5)
Sp 8 (Fig. 6H)	10&120m (NW-SE)	Velocity(m/s)	500 - 600	1400 - 1500	2800 - 3000
		Thickness(m)	1.2 - 2.5	12 - 19	------
		Top of layer (m)	19 - 22	18.5 - 21	1.5 - 5
Integrated geology and GSL			**UCWD**	**CWD**	**S.S**

Explanation:
Sp is the spread,
GI is the geophone interval,
SL is the spread length and
DS is the direction of spread.

Interpreted geology:
UCWD is the Unconsolidated Wadi Deposits.
CWD is the Consolidated Wadi Deposits.
S.S is the Sandstone layer.

The measured apparent resistivities were then presented in a contoured pseudo section, which reflect qualitatively the spatial variation in resistivity in the vertical cross-section (Griffiths and Turnbull, 1985). Therefore, the interpretation of VES data was carried out using the subsurface true resistivity contour sections (Figs. 8A and 9A) and the geoelectric cross sections (Figs. 8B and 9B), as well as the individual soundings. Careful examination of the subsurface sections can provide useful information about the subsurface lithology, structure and groundwater occurrence. It can also give additional information about the lateral discontinuities in subsurface lithology (Sadek et al., 1989).

Two geoelectric cross sections were constructed, which illustrate the distribution of the different geoelectric layers in the studied area (Fig. 3). A-A\ and B-B\ sections will be illustrated hereafter. It is worth mentioning that, the first geoelectric layer (unconsolidated Wadi sediments) is very thin and highly resistive layer. Its thinning character causes it to be unrecognizable in the 2D geoelectric cross section. So, to avoid misinterpretation, the first layer (unconsolidated sediments) and the second layer (consolidated sediments) were joined together, representing Wadi sediments in the integration of VES data with both the seismic and well logging data.

The studied area could be subdivided into two zones based on the difference in their resistivities, the northern, central and southern parts. The first geoelectric cross section, A-A\ (Fig. 8) passes through VES 1, 3 and 5 from the northwest to the southeast. The first zone of soundings 1, 3 and 5 reflects the presence of four geoelectric layers. The first and second layers (Wadi sediments) attain average thicknesses of about 8 m and 28 m respectively. The third and fourth layers represent the fractured porous rock at an average depth of 21 m.

The second zone is located deeper in VES 3 and 5 than VES 1. This zone may represent the beginning of the aquifer, because its resistivity ranges between 8 and 22 Ohm.m, so, it represents the promising layer for groundwater accumulation. Structurally, the two normal faults (F_1 and F_2 (Fig. 8 and 9)) cause of the down-faulting of the block at the central part. It represents a graben structure. The two bounding faults of the graben block are trending in the SE and NW directions.

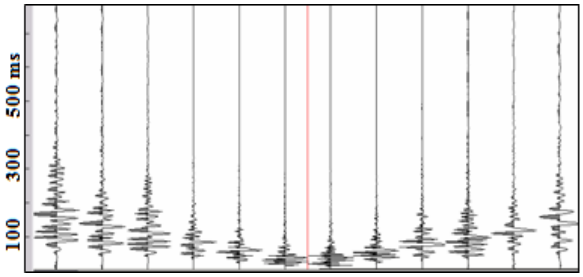

Fig. 5A: Seismogrm of split shot of the first spread.

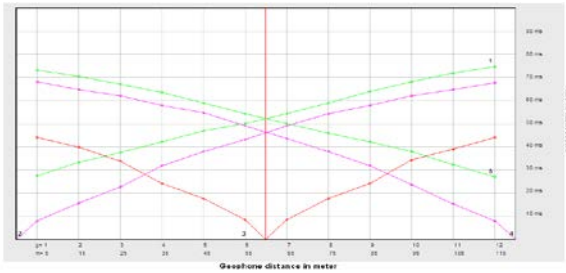

Fig. 5B: Time–Distance curve of spread (1) in the spot area.

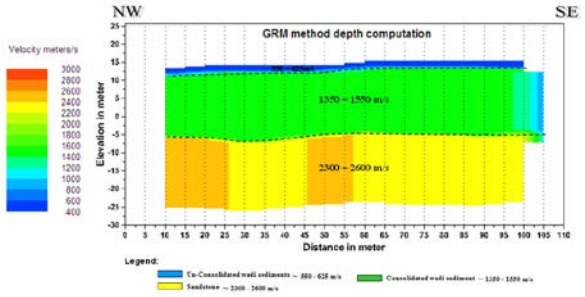

Fig. 6A: Geoseismic cross section of spread (1) by GRM.

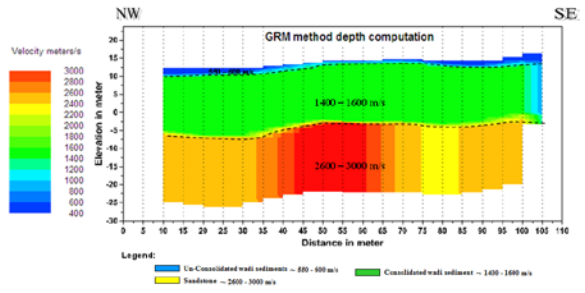

Fig. 6B: Geoseismic cross section of spread (2) by GRM.

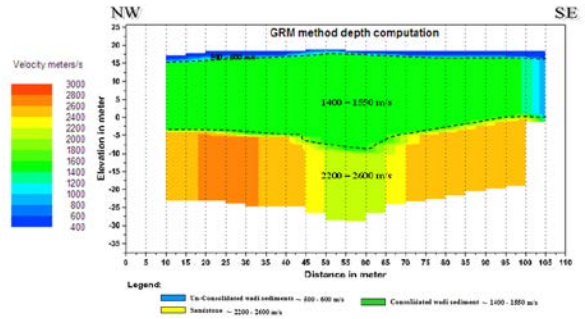

Fig. 6C: Geoseismic cross section of spread (3) by GRM.

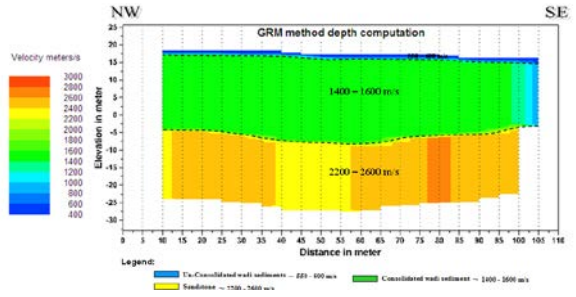

Fig. 6D: Geoseismic cross section of spread (4) by GRM.

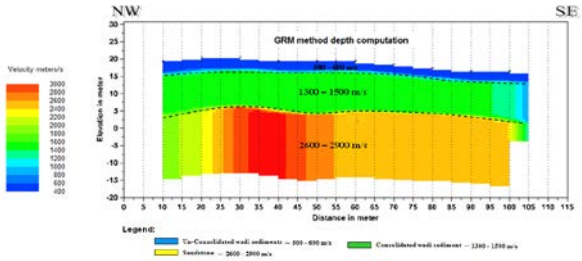

Fig. 6E: Geoseismic cross section of spread (5) by GRM.

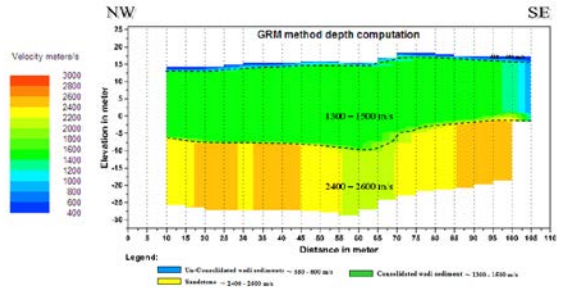

Fig. 6F: Geoseismic cross section of spread (6) by GRM.

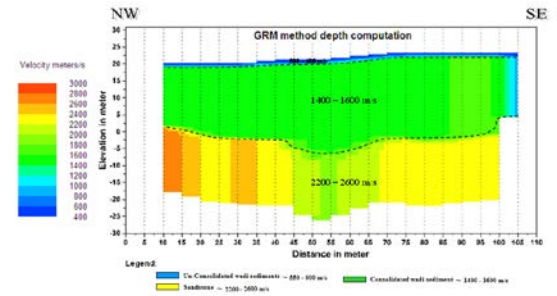

Fig. 6G: Geoseismic cross section of spread (7) by GRM.

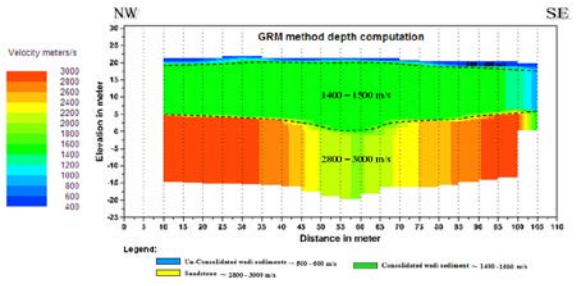

Fig. 6H: Geoseismic cross section of spread (8) by GRM.

Table 3: Resistivity parameters of geoelectric layers from Resist layering program (Velpen, 1988).

VES No.	Parameters	Geoelectric Layers			
		1	**2**	**3**	**4**
VES 1	ρ (Ohm.m)	839.6	15.8	6	22.1
	h (m)	1	6.7	43.7	-
	d (m)		1	7.2	51
VES 2	ρ (Ohm.m)	3655	700	100	21
	h (m)	3	9	54.5	-
	d (m)		3	12	66
VES 3	ρ (Ohm.m)	1429	60.4	15.8	9.6
	h (m)	3.8	19.9	85.8	-
	d (m)		3.8	23.7	110
VES 4	ρ (Ohm.m)	2036	244	26.3	70.8
	h (m)	2	9.5	93.8	-
	d (m)		2	11.5	105
VES 5	ρ (Ohm.m)	444.2	118.7	18	7.8
	h (m)	1.6	24.9	49.5	-
	d (m)		1.6	26.4	75.9
Explanation: ρ is the true resistivity value, h is the thickness of layer and d is the depth of layer.					

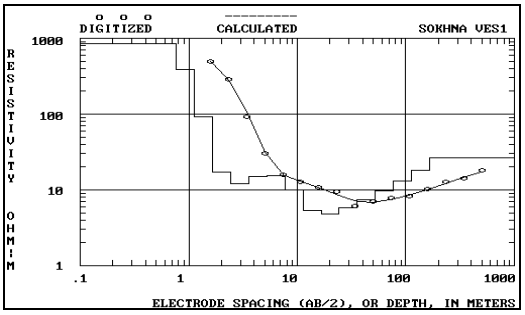

Fig. 7A: Geoelectric multi-layer modeling of VES (1) using Ato program (Zohdy, 1989) as an example.

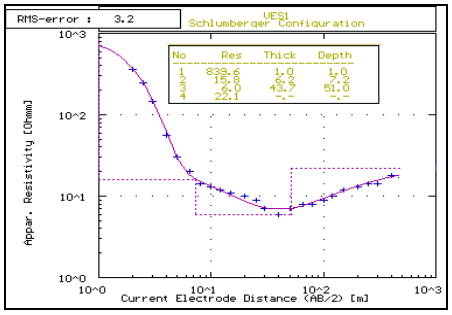

Fig. 7B: Geoelectric layer modeling of VES (1) using Resist (Velpen, 1988).

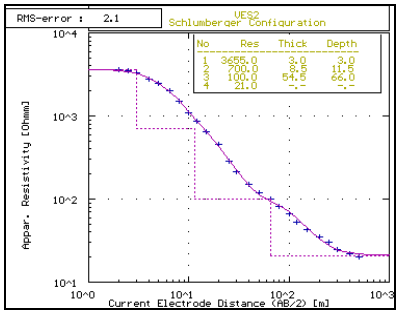

Fig. 7C: Geoelectric layer modeling of VES (2) using Resist (Velpen, 1988).

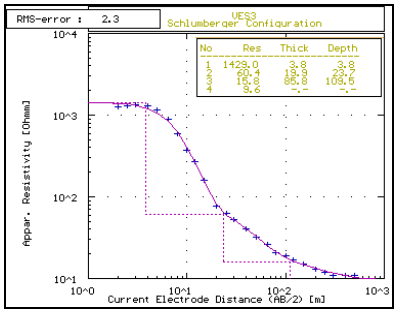

Fig. 7D: Geoelectric layer modeling of VES (3) using Resist (Velpen, 1988).

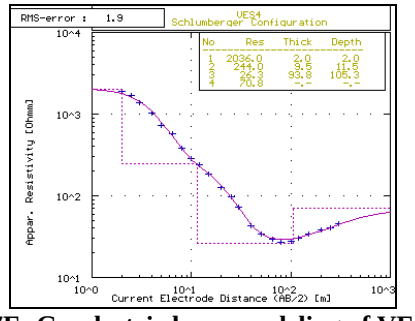

Fig. 7E: Geoelectric layer modeling of VES (4) using Resist (Velpen, 1988).

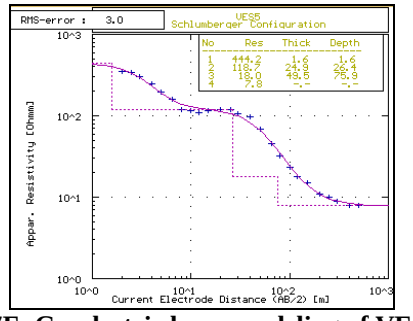

Fig. 7F: Geoelectric layer modeling of VES (5) using Resist (Velpen, 1988).

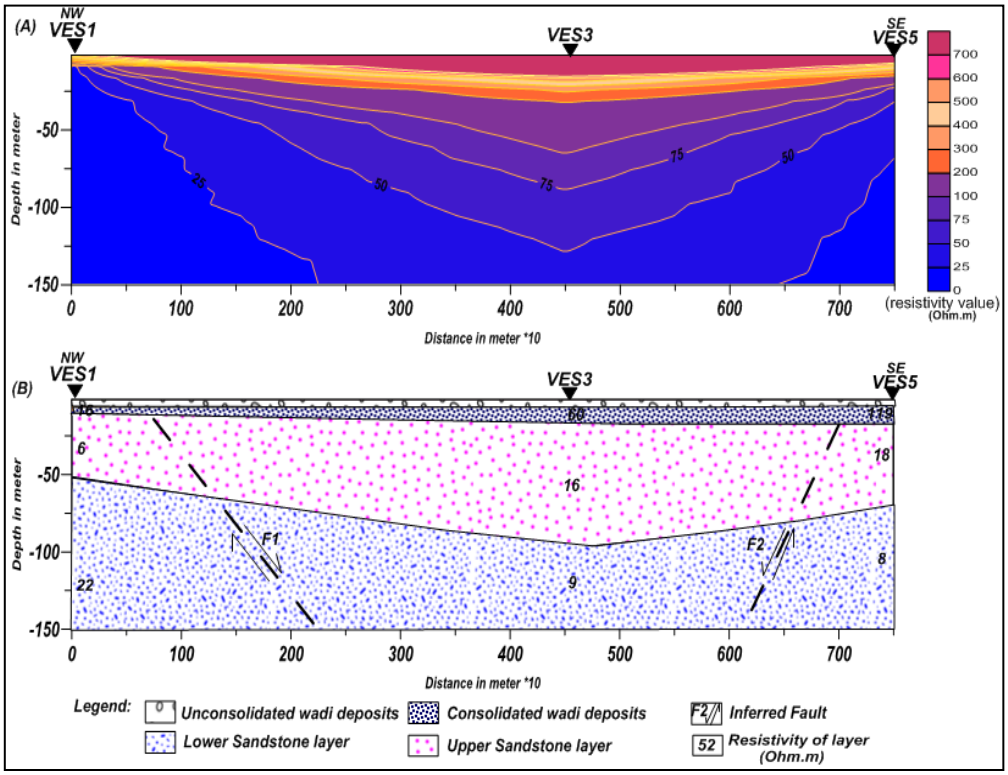

Fig. 8: (A) Subsurface true resistivity contour section A-A\ and (B) 2D geoelectric cross section A-A\ passing through VES 1, 3 and 5.

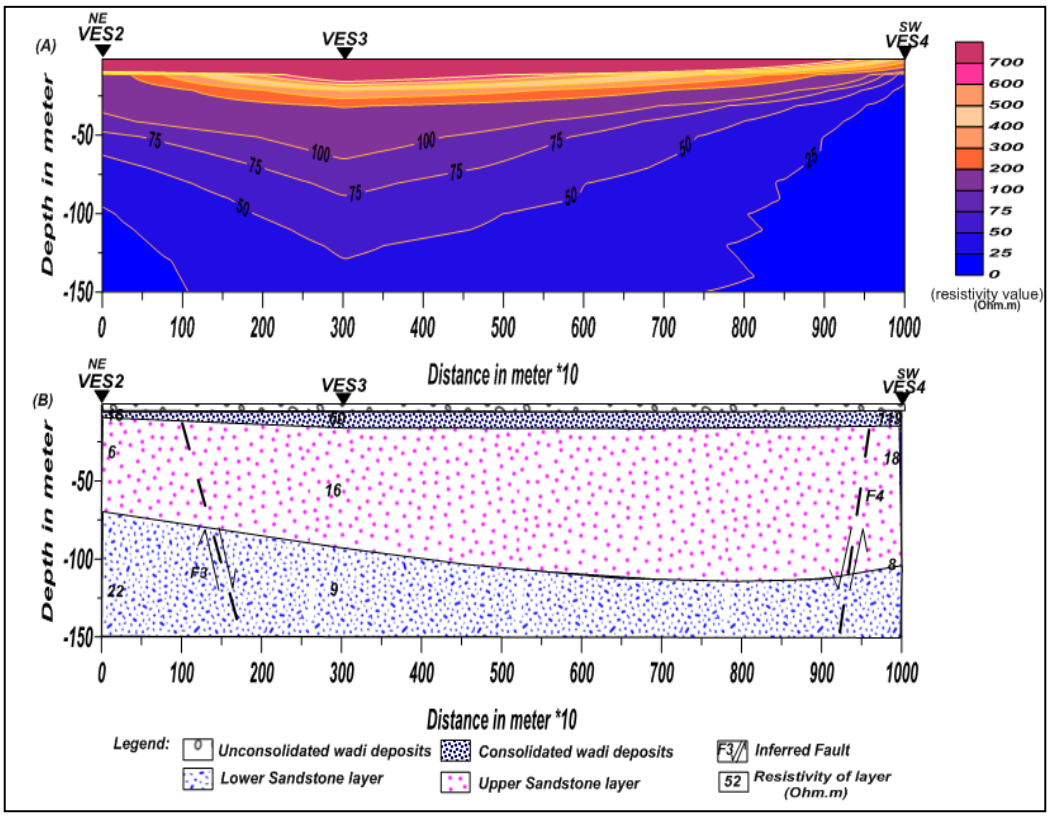

Fig. 9: (A) Subsurface true resistivity contour section B-B\ and (B) 2D geoelectric cross section B-B\ passing through VES 2, 3 and 4.

Meanwhile, the second geoelectric cross section, B-B\ (Fig. 9) passes through VES 2, 3 and 4 from the northeast to the southwest of the studied area. The layering models of the soundings 2, 3 and 4 reflect the presence of four geoelectric layers. The combination of the first and second layers show a thicknesses of 14 m, 28 m and 13 m respectively, while the third and forth layers represent the rock containing underground water.

The groundwater aquifer in the studied area is mainly composed of two different layers with different characteristic features, taking into consideration the groundwater movement and the different factors affecting this movement, such as the dipping of layers and their porosities. Structurally, two normal faults (F_3 and F_4) cause the down-faulting the block in the SW direction.

Well logging measurements included: natural gamma ray (GR), self potential (SP), electric resistivities (16″ and 64″), as well as density and neutron logs. Figures (10A to 10D) show that the well logging data of these drilled wells through out the examined area. These four figures indicate that, surface of groundwater is thought to be at 100 m depth at least.

Well No. 1 (Fig. 10 A) is composed mainly of a sandstone section which exceeds 100 m, as well as some Wadi sediments of less than 10 m at the top. The low intensity gamma ray log indicates a clean formation that is of very low radioactivity. The electrical resistivity logs confirm the occurrence of a good aquifer, where the measurements ranges about 15 Ohm.m and the water level started below 17 m, as was indicated and confirmed from both neutron and resistivity curves.

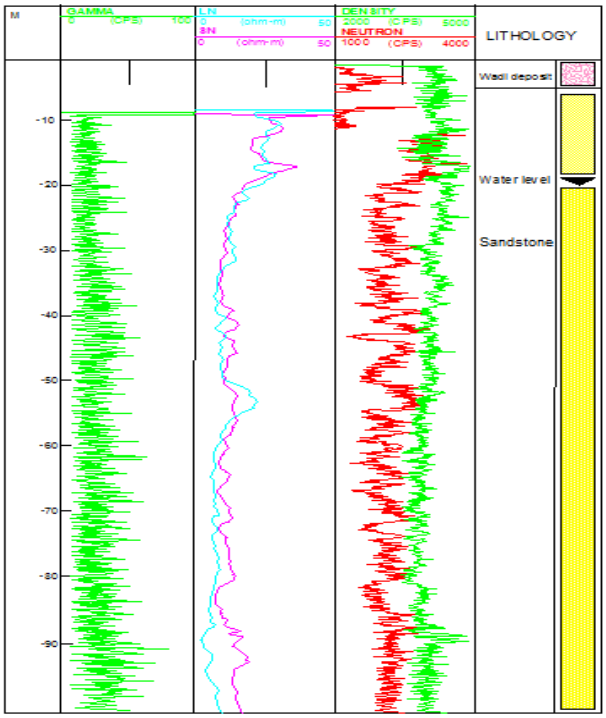

Fig. 10A: Well logging data of the upper part of well No.1.

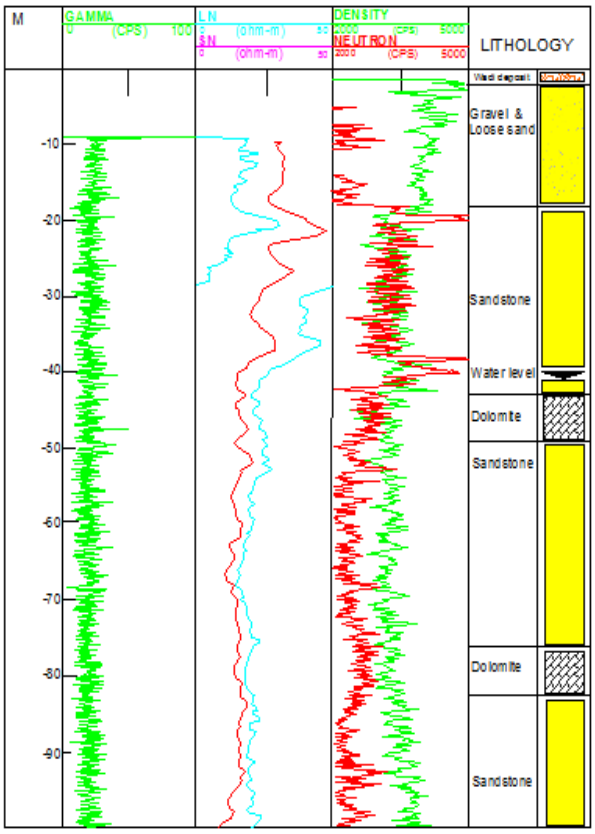

Fig. 10B: Well logging data of the upper part of well No.2.

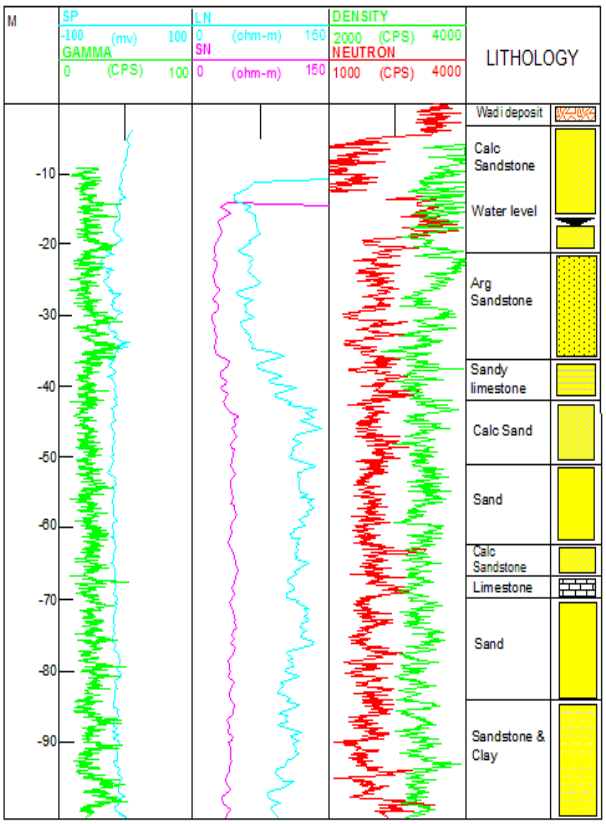

Fig.10C: Well logging data of the upper part of well No.3.

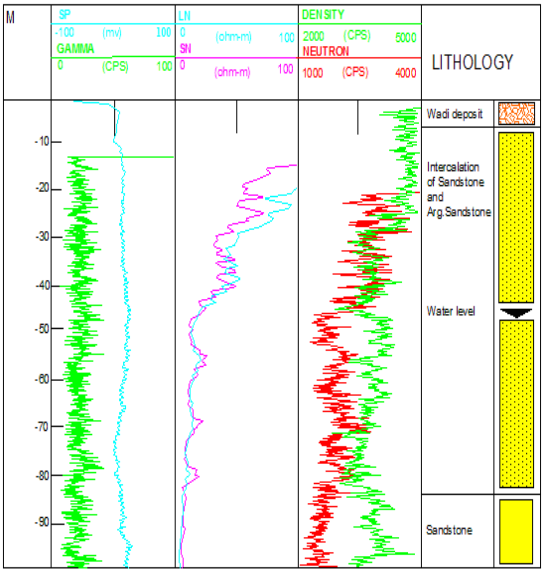

Fig. 10D: Well logging data of the upper part of well No.4.

The wire-line logging of the second well yielded at direct indication for both lithology and fluid content, in which the well penetrated Wadi sediments, gravel, loose sands and a long sandstone section, interbedded, sometimes with dolomites. The target aquifer in the well area was met at 40 m, which was confirmed with resistivity logs (around 20 Ohm.m) and neutron log (40 m depth). The aquifer represents a clean fresh water-bearing formation, which was confirmed by natural gamma logging (Fig. 10B). the water may prove to be potable (drinkable).

Lithologically, the third well (Fig. 10C) is composed of a sandstone section below Wadi weathered sediments. This sandstone cement is calcareous, becoming argillaceous in parts and interbedded with limestone in others, The electric log suite can be interpreted from the long normal resistivity (LN) 64″ curve which is relatively lower than the other wells, giving rise to120 Ohm.m. Meanwhile, the short normal resistivity (SN) 16″ reaches more than 40 Ohm.m. These values indicate perfect fresh-water aquifer that below 15 m depth. Neutron and resistivity curves confirmed this water table depth. The gamma ray log shows a clean formation at different depths in this well.

The fourth well, penetrates Wadi deposits and along a sandstone section becoming argillaceous in some intervals. At a depth of 45 m, the water table is started, which indicated from both neutron and resistivity curves. The formation shows very low radioactivity, which is considered clean as far as radioactivity is concerned. The resistivity logs indicate a saline water sandstone reservoir, in which the measurements are less than 20 Ohm.m. The formations show very low radioactivity, which is considered clean formations from radioactive materials.

The integrated seismic refraction profiles, VES and well logging techniques showed that the aquifer is a Quaternary alluvial sediments aquifer, which consists mainly of gravels, sands and clays that is underlain by sandstone. The northern part of the studied area includes VES Nos 1 and 2, as well as wells Nos 1 and 4. The studied area shows good agreement in the average level of water table of 17 m depth in VES 2 and in well No 1. Nevertheless, in case of VES No 1 and well No 4, the water table is noticed at an average depth of 45 m for the fourth geoelectric layer and the fourth well. The central part of the studied area included VES Nos 3 and 5, well No. 3 and eight seismic spreads. The water table was noticed at 11 m under VES 3, from 7 to 14 m in the seismic spreads, and 15 m in well No. 3. The southern part of the studied area is represented by well No. 2 and VES No. 4. It was found that, the static water table was detected at 27 m depth in VES No. 2 and 40 m in the drillhole 2. The total saturated thickness of the unconfined aquifer reaches more than 55 m.

CONCLUSION

A geophysical survey was planned and executed, which aims to integrate seismic refraction spreads, resistivity soundings and well logging data to delineate the subsurface geologic and hydrogeologic conditions of the groundwater status Ain Alsokhna area, West Gulf of Suez, Northern Eastern desert, Egypt. Inversion of seismic refraction data revealed that the second layer has P-wave velocity of about 1300-1600 m/s and may be considered a good indicator to ground water table in the studied area.

The application of geoelectric study showed that the sandstones in the area are highly fractured and filled with water at depths of 11 to 26 m. Resistivity sounding inversion data indicated that the aquifer possesses a resistivity range of 6-100 Ohm.m. The studied area could be subdivided into two zones which are differing in their resistivities and depths. This study also proved that, the deepest subsided block, which involves VES 3, occupies the central part of the studied area. These geoelectric interpretation results were confirmed by the drilled wells data of the drill hole No. 3 at which VES 3 site was chosen.

Drilled well results were found throughout the studied area and near to the locations of VES, supported the results of seismic refraction and resistivity sounding. The depth of the surface of groundwater increased towards the northeastern and southwestern parts of the studied area. Meanwhile, it decreased towards the northwestern and central parts. The very low radioactivity measured in the logs indicated that the aquifer is clean from this point of view.

Acknowledgement:

We are indebted to Prof. Dr. Sharaf El Dein Mahmoud Sharaf El Dein, Professor of Geophysics, Geophysics Department, Faculty of Science, Cairo University, Egypt, for his cooperation, cordial relation, continuous encouragement, advice and his effort in facilitating and revision this study.

REFERENCES

Abdellatif, T.A., Galal, G.H. and Yousef, A.M.A., 1997, Structural and lithological impact on the ground water occurrences along Wadi El Naqra-Wadi Bedaa area. Proc 15th An. Meet., Egypt, Geoph. Soc (EGS), pp.107-124.

Abuelata, A.S. and Hassanein, A.G., 1990, Comparative study of the geoelectric characteristics and water qualities in the Cairo-Suez and Cairo-Sokhna roads, Eastern Desert, Egypt. Mansoura Sci. Bull., Fac. Sci., Mansoura University, Egypt V.17 No1, Supplement, pp.511-532.

Abu-Elenain. F.M. and Ismaeil. A.S, 1995, Petrography, geochemistry and depositional history of the Eocene rocks in the area between Northern Galala and Gabal Ataqa, Western Gulf of Suez, Egypt. Annals Geol.Suv.Egypt, Vol.XX ,pp.551-576.

Bernard, J., 2003, Short note on the principles of geophysical methods for groundwater investigations. www.Terraplus.com (info@terraplus.com).

Conoco, 1987, Geological map of Egypt, Scale 1:500,000, NH36 SW-BENI SUEF sheet.

Elbehiry, M.G., Shideed, A.G. and Elhusseiny, M.S., 2004, Geographic Information System and remote sensing application for water resources: Wadi Ghoweibba Basin, West Gulf of Suez, Egypt. 7th Internat. Conf. on Geol. Arab World, Cairo Univ, Egypt, p.22.

Eldiasty, M.I., Elhakeim, B.E.A. and Saber, H.S.M., 1981, carried out some recent geophysical well logging investigations in mining and ground water prospect in Ain El-Sokhna, Abu Tartur and Maghara.which, different bore hole are drilled in the area to study the geological section and geophysical parameters.

Galfi J. and Palos M., 1970, Bulletin of the Intern Assoc. of Scientific Hydrology, XV, pp. 41-48.

Griffiths, D. and Turnbull, J., 1985, A multi-electrode array for resistivity surveying. First Break, 3, No. (7), .pp:16–20.

Reynolds, J. W., 1997, An introduction to applied and environmental geophysics. New York, USA, 796p.

Sadek, H.S., Soliman, S.A. and Abdulhady, H.M., 1989, Correlation between different models of resistivity sounding data to discover new fresh water fields in Elsadat City, Western Desert, Egypt. Proc. of the 7th International Mathematical Geophysics Seminar, Free University of Berlin, Western Germany 8-11 Feb., 1989, pp. 329-346.

Said, R., 1990, The geology of Egypt. Rotterdam Pup.Co,722p.

Salem, A.S., 1988, Geological and hydrogeological studies on the area between Gabal Ataqa and Northern Galala plateau, Egypt. Ph.D., Fac .Sci, Geol. Dept, Zagazig Univ, Egypt, 271p.

Velpen, B.P.A., 1988, Resist program, V. 1.0. M.Sc Research project, ITC, Holland.

Winsism, V., 2009, http://www.wgeosoft.h Seismic refraction processing software.

Youssef, M.I. and Abdelrahman, M.A., 1978, Structural map sensing of the area between Gabal Ataqa and northern Galala plateau, Gulf of Suez region, Egypt.Tenth Arab petroleum conference, Trippoli, Libya, 135(C-3) 8p.

Zohdy, A.A.R., 1974, Use of Dar Zarrouk curves in the interpretation of vertical electrical sounding data; U.S. Geol. Surv. Bull., 1313-D, 41 p.

Zohdy, A.A.R. and Bisdorf, R., 1989, A program for automatic processing and interpretation of Schlumberger sounding curves in Quick Basic 4.0. U. S. Geological Survey, Open - File Report, 89-137, 67 p.